Bull. Mater. Sci., Vol. 40, No. 1, February 2017, pp. 171–175. © Indian Academy of Sciences.
DOI 10.1007/s12034-017-1365-5

Na-doped $LiMnPO_4$ as an electrode material for enhanced lithium ion batteries

K RAJAMMAL[1], D SIVAKUMAR[2], NAVANEETHAN DURAISAMY[1,*], K RAMESH[1] and S RAMESH[1]

[1]Center for Ionics University of Malaya, Department of Physics, University of Malaya, Kuala Lumpur 50603, Malaysia
[2]Faculty of Mechanical Engineering, University Technical Malaysia Melaka (UTeM), 76100 Durian Tunggal, Malaysia

MS received 20 October 2015; accepted 27 June 2016

Abstract. **We report the influence of sodium (Na)-incorporated lithium manganese phosphate as an active material on its performance in electrochemical study for energy storage application. $Li_{1-x}Na_xMnPO_4$ with different mole ratios ($0.00 \leq x \leq 0.05$) of sodium is synthesized via a simple sol–gel method. The discharge capacity of $Li_{1-x}Na_xMnPO_4$ varies with respect to mole ratios of sodium incorporated. The maximum discharge capacity of 92.45 mAh g^{-1} is observed in $Li_{0.97}Na_{0.03}MnPO_4$, which is higher than that of pristine $LiMnPO_4$ and other Na-incorporated $LiMnPO_4$. The maximum cyclic stability is found to be 84.15% up to 60 cycles. These results demonstrate that $Li_{0.97}Na_{0.03}MnPO_4$ plays a significant role in future energy storage application.**

Keywords. **$LiMnPO_4$; sodium doping; cathode materials; electrochemical study; lithium ion batteries.**

1. Introduction

Hybrid electric vehicles require lithium rechargeable batteries because of their excellent power density and long life time [1]. Cathode is the most important element within the lithium batteries, which gives significant impact on capacity and electrochemical performance. Lithium manganese phosphate ($LiMnPO_4$) is mainly focused as a suitable candidates in the olivine group among $LiFePO_4$, $LiCoPO_4$ and $LiNiPO_4$ for cathode application [2,3]. In $LiMnPO_4$, the P–O covalent bond enables good thermal and cycling stability [4,5]. The theoretical energy density of $LiMnPO_4$ is 701 Wh kg^{-1} with poor lithium diffusion and low electronic/ionic conductivity, which affect the electrochemical property [6,7].

Various synthesis methods are developed to overcome these drawbacks, which focus mainly on particle size control [8–10], carbon coating [11,12] and cation doping [13–15]. Moreover, the surface morphologies are an essential factor for electrochemical properties. Recently haemoglobin-like $LiMnPO_4$ microspheres were prepared for better electrochemical activity due to presence of three-dimensional (3D) hierarchical structures [16]. $LiMnPO_4$ nanorods (<30 nm) are produced by controlling boiling temperature, solvent, concentration of surfactants, reaction temperature and time [17]. Cui *et al* [18] reported that irregular flaky shaped $LiMnPO_4$ is achieved by a hollow-sphere Li_3PO_4 precursor, which is used to control the particle growth of $LiMnPO_4$. Also, Doi *et al* [9] stated that by controlling particle size, the diffusion and conduction path are shortened, which lead to improvement of conductivity. On the other hand, Nam *et al* [19] reported that the carbon-coated nanostructured $LiMnPO_4$ via combination of spray pyrolysis and dry ball milling revealed good electrochemical properties at high temperature and high charge/discharge rate of 2C. Herein, carbon layer is also found to be effectively suppress the crystal growth during heat treatment, resulting in a significant improvement of cycling performance [11].

Cation doping in $LiMnPO_4$ is found to be an alternative method to upgrade ionic conductivity [13]. Recent work indicated that cesium (Ce)-doped $LiMnPO_4$ led to easy diffusion of lithium ion in bulk materials [20]. In another work, electrochemically inactive cations were replaced partially for Mn; thus $LiMn_{0.88}Mg_{0.1}Zr_{0.02}PO_4$ exhibited high discharge capacity (134.0 mAh g^{-1}) and lower irreversible capacity loss [21]. This enhancement is accredited to good kinetic properties due to the reduced distortion of local structure. Co-substituted iron (Fe) and magnesium (Mg) evenly spread over $LiMnPO_4$, leading to shrinkage of crystal lattice [22]. Considering this fact, this work is an effort to improve $LiMnPO_4$ by partial natrium substitution on lithium sites. The ionic radius of natrium (0.098 nm) is bigger than that of lithium (0.076 nm); thus it is highly possible to increase the interlayer space for facile lithium movement during intercalation and deintercalation processes [23,24]. Na element is inexpensive, ample and environment friendly [23]. Several attempts have been done to improve electrochemical performance of cathode materials by partial natrium doping. $Li_{1.17}Na_{0.03}[Co_{0.13}Ni_{0.13}Mn_{0.54}]O_2$ demonstrated high discharge capacity, larger coulombic efficiency, enhanced rate capability and cycling stability as compared

*Author for correspondence (naveennanoenergy@gmail.com)

with $Li_{1.17}Na_{0.03}[Co_{0.13}Ni_{0.13}Mn_{0.54}]O_2$ [24]. Chen *et al* [25] reported that Na^+ substitution for Li^+ minimizes cation mixing, improves reversibility and restricts charge transfer impedance during cycling.

The present work reports the preparation and electrochemical characterizations of $Li_{1-x}Na_xMnPO_4$ with different mole ratios of sodium, $x = 0.00$, 0.01, 0.02, 0.03, 0.04 and 0.05. To the best of our knowledge, partial Na^+ substitution for Li^+ site has not been focused for $LiMnPO_4$-based energy storage application.

2. Experimental

2.1 *Materials*

Lithium acetate ($LiC_2H_3O_2$) and sodium acetate ($C_2H_3NaO_2$) were purchased from Aldrich. Manganese acetate $Mn(CH_3COO)_2{\cdot}4H_2O$ and ammonium dihydrogen phosphate ($NH_4H_2PO_4$) were obtained from Friendmann Schmidt.

2.2 *Synthesis process*

$Li_{1-x}Na_xMnPO_4$ ($0.00 \leq x \leq 0.05$) was synthesized by the sol–gel method. Lithium acetate, sodium acetate and manganese acetate were dissolved together with ammonium dihydrogen phosphate in the molar ratios $1{:}x = 0.00$, 0.01, 0.02, 0.03, 0.04, 0.05:1:1. Dissolution of this mixture was done in distilled water under magnetic stirring at 120°C and maintained until a solid product was formed. Finally, the obtained solid material was sintered at 700°C for 3 h.

2.3 *Structural and electrochemical characterizations*

XRD measurements were obtained using a Siemens D 5000 diffractometer with Cu-Kα radiation ($\lambda = 1.54060$ Å). The diffraction intensity was recorded in the range 10–80° with step size 0.02°. The surface morphology of synthesized samples was examined by field emission scanning electron microscopy (microscope model JSM 7600-F).

To prepare thin films, 80 wt% of active materials ($Li_{1-x}Na_xMnPO_4$) was mixed with 20 wt% of carbon, 20 mg of $Li_{1-x}Na_xMnPO_4$/C and 8 mg of teflonized acetylene (TAB) in ethanol medium, followed by pressing on a stainless steel mesh and then dried at 120°C for 12 h. Then, the cell was assembled in an argon atmosphere using $Li_{1-x}Na_xMnPO_4$-based electrode as a cathode, lithium metal as an anode and 1 M $LiPF_6$ dissolved in a mixture of ethylene carbonate (EC)/dimethyl carbonate (DMC) (1:1 in volume) as an electrolyte. Cyclic voltammetry tests were carried out using an auto lab in the potential range of 2.5–4.5 V. All the samples were charged at 1.0 mA and discharged at 0.5 mA between 2.5 and 4.5 V on a Neware battery system (AC 10 mV). Electrochemical impedance spectroscopy (EIS) tests were carried out using a Gamry instrument in the frequency range of 0.05 Hz–10 kHz.

3. Results and discussion

The structural crystallinity was examined using the XRD pattern. Figure 1 presents the patterns of pristine $LiMnPO_4$ and $Li_{1-x}Na_xMnPO_4$ ($0.00 \leq x \leq 0.05$). The observed diffraction peaks at $2\theta = 20.4$, 25.1, 29.1 and 35.07° correspond to (011), (111/021), (200/121) and (131) planes, respectively. This was well indexed to the orthorhombic structure of $LiMnPO_4$ (JCPDS No. 33-804) with space group of Pnmb [15,16]. However, the lattice parameters varied due to Na metal doping in $LiMnPO_4$, which are given in table 1.

Both *a* and *c* lattices expand with increasing Na metal doping. *c*-Axis enlargement indicates the expansion of Li pathway within the structure [26]. Also, the enlargement in *a* site provides smoother Li diffusion during the intercalation process. Moreover it has been proved by the simulation method that Li ion moves through the *a*-axis due its lower activation energy, which was supported by Oh *et al* [27]. Therefore, this provides smoother Li diffusion during the intercalation process, suggesting enhanced electrochemical performance [24].

FESEM analysis was used to study the surface morphology of synthesized samples. Figure 2 displays surface morphology of $Li_{1-x}Na_xMnPO_4$ ($0.00 \leq x \leq 0.05$) particles formed at 700°C (calcination temperature). Agglomeration

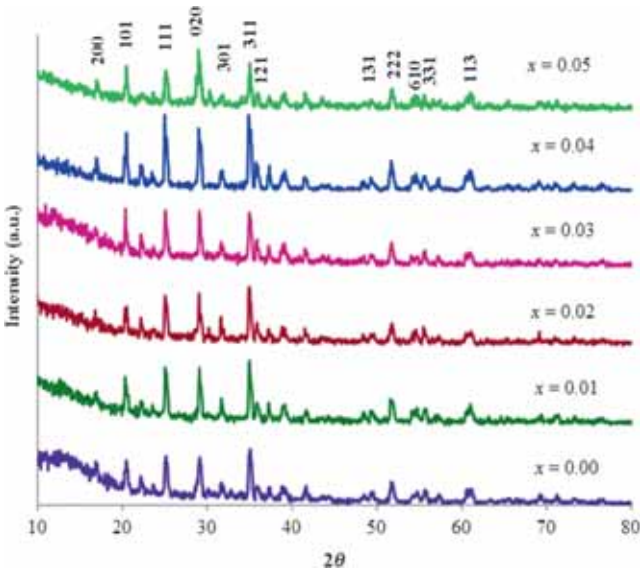

Figure 1. XRD of $Li_{1-x}Na_xMnPO_4$ ($0.00 \leq x \leq 0.05$) sintered at 700°C.

Table 1. Calculated lattice parameters of $Li_{1-x}Na_xMnPO_4$ ($0.00 \leq x \leq 0.05$).

x in $Li_{1-x}Na_xMnPO_4$	a (Å)	c (Å)
0.00	6.117	4.718
0.01	6.122	4.734
0.02	6.126	4.740
0.03	6.131	4.750
0.04	6.136	4.765
0.05	6.137	4.784

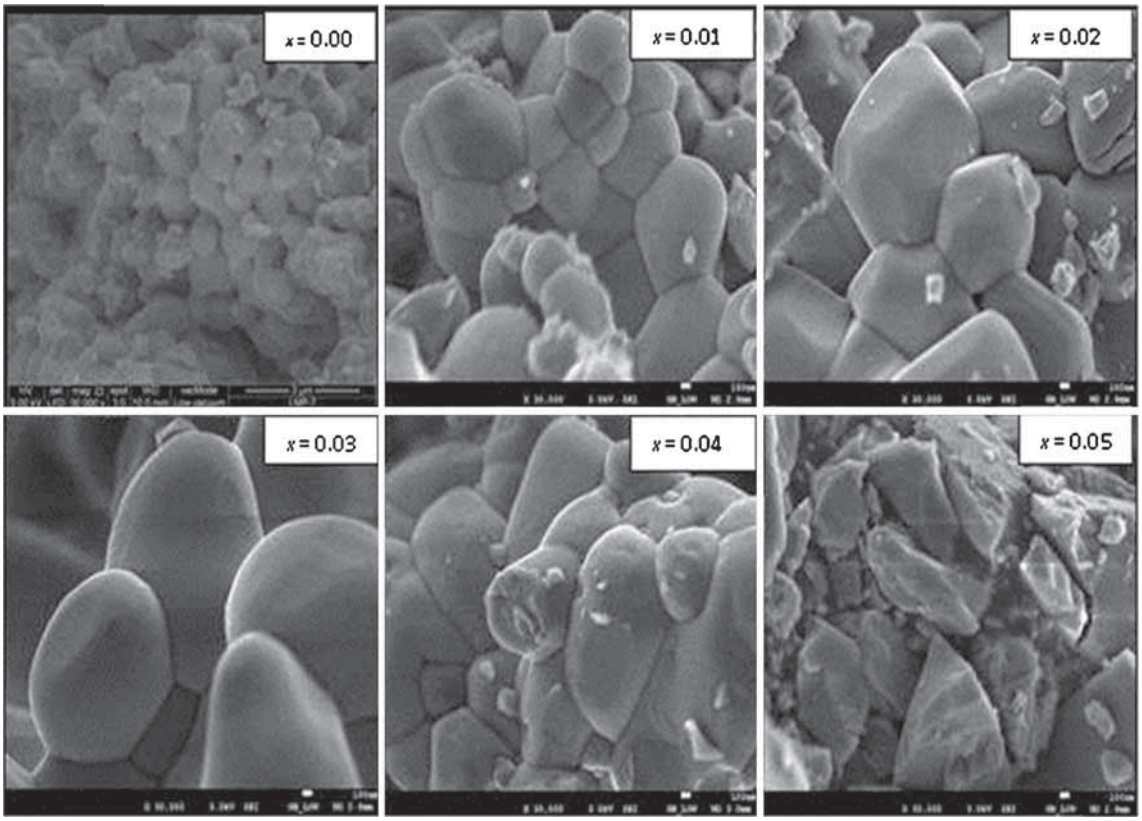

Figure 2. FESEM images of $Li_{1-x}Na_xMnPO_4$ ($x = 0.00$, 0.01, 0.02, 0.03, 0.04 and 0.05) particles.

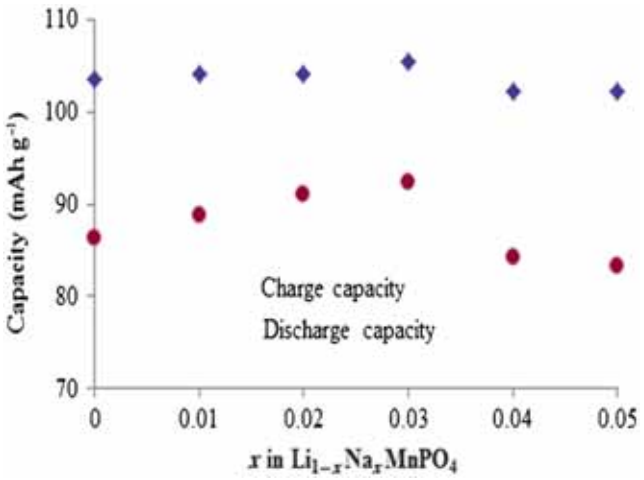

Figure 3. Initial charge and discharge capacities of $Li_{1-x}Na_x$ $MnPO_4$ particles.

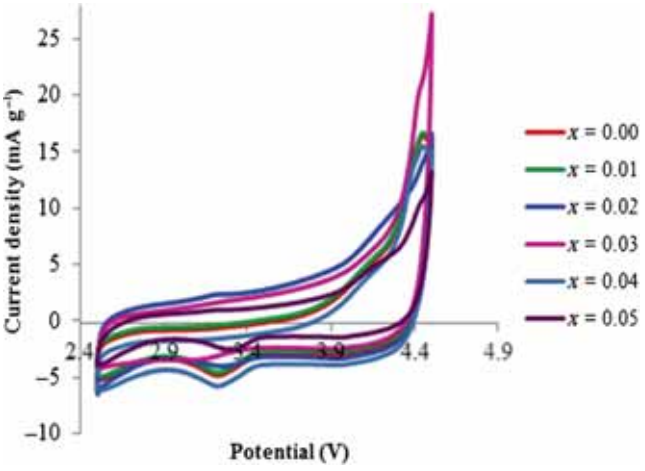

Figure 4. Cyclic voltammetry of $Li_{1-x}Na_xMnPO_4$ ($0.00 \leq x \leq 0.05$) samples at scan rate of 0.2 mV s^{-1}.

that occurs from $x = 0.00$ until $x = 0.03$ was higher as compared with $x = 0.04$ and $x = 0.05$. Agglomerated particles and individual particles are present together in the samples and agglomerated particles are formed by smaller individual particles.

Figure 3 clearly displays that the initial charge and discharge capacities increase from $x = 0.00$ to $x = 0.03$ and then tend to decrease until $x = 0.05$. Irreversible capacity loss decreases with addition of Na^+ in the Li^+ site. Less irreversible loss observed in $Li_{0.97}Na_{0.03}MnPO_4$ was found to be (4.1 mAh g^{-1}) lesser than that of pristine $LiMnPO_4$ (11.5 mAh g^{-1}). Also, the maximum capacity values were recorded at $x = 0.03$. A similar pattern was observed for continuous electrochemical cycling. Therefore, the enhanced cycling performance is attributed to the structure stabilization with Na^+ ions, which act as a pillar [20,21].

Cyclic voltammograms for $Li_{1-x}Na_xMnPO_4$ ($x = 0.00$, 0.01, 0.02, 0.03, 0.04 and 0.05) are shown in figure 4.

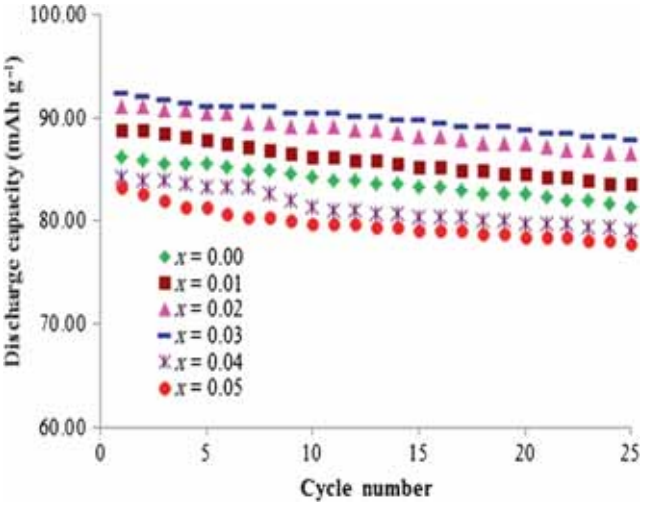

Figure 5. Discharge capacities of $Li_{1-x}Na_xMnPO_4$ ($0.00 \leq x \leq 0.05$) particles at current 0.5 mA.

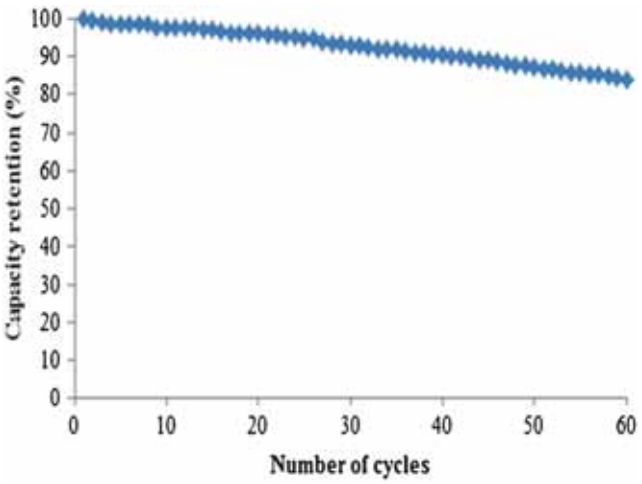

Figure 6. Capacity retention of $Li_{0.97}Na_{0.03}MnPO_4$ at current 0.5 mA.

Cyclic voltammetry depicts similar patterns as the Na substitution varies at a minor level. Interestingly, anodic and cathodic peaks become sharper as Na substitution level rises to $x = 0.03$ in $Li_{1-x}Na_xMnPO_4$. This clearly denotes partial substitution of Li by Na, which increases peak currents, resulting in the improvement of electrochemical properties [28].

Figure 5 illustrates the discharge capacities of $Li_{1-x}Na_xMnPO_4$ ($0.00 \leq x \leq 0.05$) in the voltage range of 2.5–4.5 V at current rate 0.2C. It presents initial discharge capacities of 86.3, 88.9, 91.2, 92.4, 84.3 and 83.3 mAh g^{-1} for $x = 0.00$, 0.01, 0.02, 0.03, 0.04 and 0.05 in $Li_{1-x}Na_xMnPO_4$, respectively. At the same time, coulombic efficiency improved from 83.3% (pristine $LiMnPO_4$) to 87.6% ($Li_{0.97}Na_{0.03}MnPO_4$). Na^+ ions act as pillars, providing wider space for lithium ions movement [20,21]. This improved the intercalation and deintercalation processes within the materials and smoothened them [29]. Apart from these, Jahn Teller distortion is related to the Mn–Mn distance in the crystalline structure. Here, Na substitution made Mn–Mn distance longer as Na^+ ions are larger compared with Li^+ ions. This weakens the Jahn Teller effect and also yields strong cycling stability [30].

The mole ratio of 0.03 in $Li_{1-x}Na_xMnPO_4$ was found to be the maximum level of doping that enhances cycling properties [31]. Beyond this the addition of Na (>0.03) deteriorates the capacitive nature due to structural instability and weak electrochemical performance [30,32]. $Li_{0.97}Na_{0.03}MnPO_4$ demonstrated the maximum cycling stability compared with other samples with moderate doping of Na.

Figure 6 displays the capacity retention of $Li_{0.97}Na_{0.03}MnPO_4$ for 60 cycles. Initial charge capacity of $Li_{0.97}Na_{0.03}MnPO_4$ was found to be 105.4 mAh g^{-1}, which results in irreversible capacity of 12.9 mAh g^{-1}. Capacity retention based on initial discharge capacity reaches about 97.89% at the 10th cycle, 96.12% at the 20th cycle, 92.96% at the 30th cycle, 90.49% at the 40th cycle and 87.32% at the 50th cycle. It delivers discharge capacity of 77.80 mAh g^{-1} at the 60th cycle, which is able to retain 84.15% of its initial discharge capacity of 92.4 mAh g^{-1}.

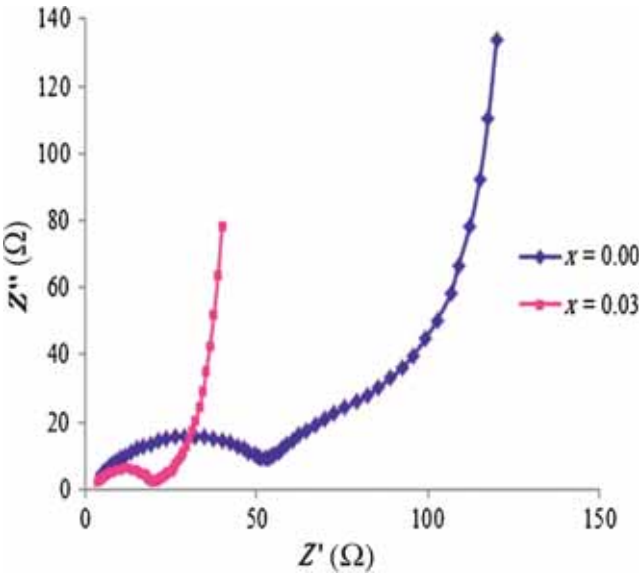

Figure 7. Impedance spectra of $LiMnPO_4$ and $Li_{0.97}Na_{0.03}MnPO_4$ from EIS measurements.

Impedance spectra of $LiMnPO_4$ and $Li_{0.97}Na_{0.03}MnPO_4$ can be observed in figure 7. It is noteworthy that semicircles of Na-substituted $LiMnPO_4$ samples exhibit smaller radius compared with $LiMnPO_4$. This ascertains increased electronic conductivity and hence facilitates smooth lithium ion movement into active materials [32]. The observed R_{ct} value for $LiMnPO_4$ is around 57 Ω, while R_{ct} of $Li_{0.97}Na_{0.03}MnPO_4$ is found to be about 19 Ω. This describes that partial Na substitution is able to reduce charge transfer resistance [25].

4. Conclusion

This work demonstrated the effect of Na doping in $LiMnPO_4$. Na of different concentrations was substituted in the

$LiMnPO_4$ system via the sol–gel method. The XRD pattern confirmed the well-indexed crystalline structure. Addition of Na ions into the crystal structure expands the Li slab space. The maximum discharge capacity of 92.45 mAh g^{-1} was achieved in $Li_{0.97}Na_{0.03}MnPO_4$, compared with pristine $LiMnPO_4$ (86.26 mAh g^{-1}), with the maximum cyclic stability of 84.15% up to 60 cycles. Irreversible capacity loss was reduced by natrium addition ($Li_{0.97}Na_{0.03}MnPO_4$ compared with pristine $LiMnPO_4$). Therefore, these experimental results suggested that superior electrochemical performance can be attained through optimizing adequate Na doping in $LiMnPO_4$ towards lithium ion battery application.

Acknowledgements

We would like to thank financial support from the University of Malaya via PPP grant PG 099 – 2014B and Fundamental Research Grant Scheme (FP012-2015A) from the Ministry of Education, Malaysia.

References

[1] Kim J, Seo D, Kim S, Park Y and Kang K 2010 *Chem. Commun.* **46** 1305

[2] Koleva V, Zhecheva E and Stoyanova R 2011 *Dalton Trans.* **40** 7385

[3] Zhang W, Shan Z, Zhu K, Liu S, Liu X and Tian J 2015 *Electrochim. Acta* **153** 385

[4] Yoshida J, Stark M, Holzbock J *et al* 2013 *J. Power Sources* **226** 122

[5] Qin Z, Zhou X, Xia Y, Tang C and Liu Z 2012 *J. Mater. Chem.* **22** 21144

[6] Aono S, Urita K, Yamada H and Moriguchi I 2012 *Solid State Ion* **225** 556

[7] Dong Y, Wang L, Zhang S *et al* 2012 *J. Power Sources* **215** 116

[8] Zhao M, Fu Y, Xu N, Li G and Gao X 2014 *J. Mater. Chem. A* **2** 15070

[9] Doi T, Yatomi S, Kida T, Okada S and Yamaki J 2009 *Cryst. Growth Des.* **9** 10

[10] Zhu K, Zhang W, Du J *et al* 2015 *J. Power Sources* **300** 139

[11] Su K, Liu F and Chen J 2013 *J. Power Sources* **232** 234

[12] Moon S, Muralidharan P and Kim D K 2012 *Ceram. Int.* **38** S471

[13] Jo M, Yoo H, Jung Y S and Cho J 2012 *J. Power Sources* **216** 162

[14] Gan Y, Chen C, Liu J, Bian P, Hao H and Yu A 2015 *J. Alloys Compd.* **620** 350

[15] Ottmann A, Jähne C, Meyer H-P and Klingeler R 2015 *Mater. Res. Bull.* **63** 6

[16] Gu Y, Wang H, Zhu Y, Wang L, Qian Y and Chu Y 2015 *Solid State Ion* **274** 106

[17] Kwon N H and Fromm K M 2012 *Electrochim. Acta* **69** 38

[18] Cui Y-T, Xu N, Kou L-Q, Wu M-T and Chen L 2014 *J. Power Sources* **249** 42

[19] Nam T, Doan L, Bakenov Z and Taniguchi I 2010 *Adv. Powder Technol.* **21** 187

[20] Kou L, Chen F, Tao F, Dong Y and Chen L 2015 *Electrochim. Acta* **173** 721

[21] Lee J, Park M, Anass B, Park J, Paik M and Doo S 2010 *Electrochim. Acta* **55** 4162

[22] Hu C, Yi H, Fang H *et al* 2010 *Electrochem. Commun.* **12** 1784

[23] Wang J, Lin W, Wu B and Zhao J 2014 *Electrochim. Acta* **145** 245

[24] He Wei, Yuan D, Qian J, Ai X, Yang H and Cao Y 2013 *J. Mater. Chem. A* **1** 11397

[25] Chen Z, Xie T, Li L and Xu M 2014 *Ionics* **20** 629

[26] Hee W, Yuan D, Qian J, Ai X, Yang A and Cao Y 2013 *J. Mater. Chem. A* **1** 11397

[27] Oh R-G, Hong J-E, Jung H-W and Ryu K-S 2015 *J. Power Sources* **295** 1

[28] Qiu B, Wang J, Xia Y, Liu Y, Qin L, Yao X and Liu Z 2013 *J. Power Sources* **240** 530

[29] Park S H, Shin S S and Sun Y K 2006 *Mater. Chem. Phys.* **95** 218

[30] Sun F and Xu Y 2014 *J. Alloys Compd.* **584** 538

[31] Gong C, Lv W, Qu L *et al* 2014 *J. Power Sources* **247** 151

[32] Hu G, Zhang M, Liang L, Peng Z, Du K and Cao Y 2016 *Electrochim. Acta* **190** 264